RSC Advances

ROYAL SOCIETY
OF CHEMISTRY

www.rsc.org/advances

Cite this: DOI: 10.1039/c0xx00000x

www.rsc.org/xxxxxx

ARTICLE TYPE

Tunable Self-Assembly Structure of Graphene Oxide/Cellulose Nanocrystal Hybrid Films Fabricated by Vacuum Filtration Technique

Qi Chen, Ping Liu, Chunrui Sheng, Lijuan Zhou, Yongxin Duan and Jianming Zhang*

Received (in XXX, XXX) Xth XXXXXXXXX 20XX, Accepted Xth XXXXXXXXX 20XX

DOI: 10.1039/b000000x

By adjusting the dispersibility of graphene oxide (GO) in cellulose nanocrystal (CNC) aqueous solution, two distinct GO/CNC hybrid films with various internal structure have been obtained via vacuum-assisted self-assembly. After reduction, thus prepared GO/CNC hybrid films respectively demonstrate high conductivity or iridescent properties.

Cellulose nanocrystals (CNCs), the nanoscale building materials isolated from native cellulose sources, have inspired vast research enthusiasm not only because of its remarkable physical and chemical properties but also for their potential application in sustainable biomaterial-based society.[1] It is well known that controlled hydrolysis of cellulose fibers with sulfuric acid is the mostly used method to generate rod-like CNCs. This strategy provides CNCs with negatively charged surfaces so that the CNCs form a stable colloidal suspension in water by the electrostatic repulsion. Thus, CNCs obtained from the sulfuric acid-catalyzed hydrolysis have been considered as a well dispersed nano-filler to prepare composites with other water soluble materials by simple solution mixing.[2]

In essence, the primary reason to utilize CNCs in composite materials is that the excellent mechanical properties of CNCs can be potentially exploited for reinforcement. However, this was only one face of the coin. The anisotropic rod-like CNCs also show the striking ability to self-organize into chiral nematic liquid crystal phase in concentrated solution, which could result in iridescent solid films after the evaporation of solvents.[3] Efforts on duplicating the chiral nematic structure appearing in CNC iridescent films, which is in relation to new designing of optically functional materials, manifest other latent applications of CNCs. For example, MacLachlan's group has recently published a series of pioneering work[4] and shown that the chiral nematic photonic properties of CNCs can be arrested in other materials by the addition of suitable precursors that are compatible with CNC self-assembly.

Of note, static solution-casting with slow solvent evaporation, which is also termed as evaporation-induced self-assembly (EISA) in some literatures,[5-6] is the general method for obtaining the CNC iridescent films. Previous reports show that the iridescence of CNC films can be tuned by changing the helical pitch of self-organized chiral nematic phase via either adding electrolytes,[7a] applying ultrasonication to the CNC dispersion,[7b] heating the CNC solution[7c] or changing the substrate[7d] and varying evaporation rate.[7c-7d] Till now, there is no report on CNC iridescent films prepared by vacuum filtration, although the method is widely used as a simple and fast way to prepare large-scale free-standing films.

In the present study, our initial purpose is to fabricate highly conductive CNC composite film with uniform dispersed graphene in CNC matrix via vacuum filtration, which is also termed as vacuum-assisted self-assembly technique (VASA). To this end, a small amount of water soluble graphene oxide (GO), the precursor of grephene, was used to incorporate with CNCs. Unexpectedly, it is the first time to find that iridescent GO/CNC hybrid films with highly ordered chiral nematic structure can be also obtained by simply controlling the dispersion method of GO in CNC aqueous solution.

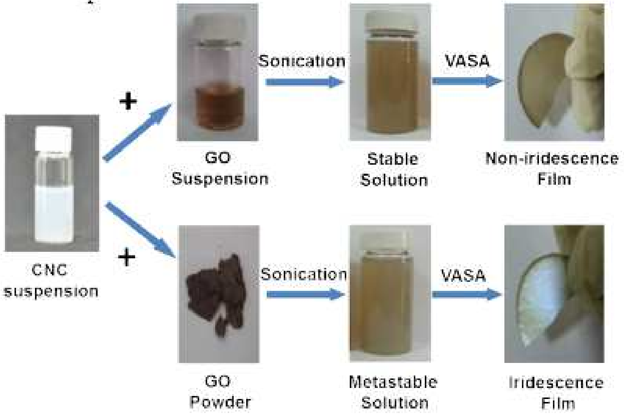

Scheme.1 Illustration of the preparation process of GO/CNC hybrid films with or without iridescence.

As illustrated in Scheme 1, the CNC suspension (pH=2; 1 wt %) produced through sulphuric acid hydrolysis of cotton linter pulp was used as the starting material to prepare GO/CNC hybrid films. The CNC suspension prepared with sulfuric acid exhibits highly colloidal stabilities even at pH around 2, which is evidenced by its zeta potential value (-41mV). Actually, CNC suspensions with pH around 2 had been used as staring material in previous studies.[4, 8] AFM morphology characterization in Fig. 1a shows that rod-like CNCs with uniform nanoscale size are successfully prepared. GO was prepared using Hummers' Method [9] and morphology data (see Fig. 1b) suggests that the GO has wide size distribution in micrometer level. In order to prepare GO/CNC solution by VASA, two dispersion methods to add small amount of GO (0.3 wt %) in CNC aqueous solution were used. One route is to prepare the well dispersed GO in deionized water firstly (the pH and zeta potential of resulted GO solution are around 3.5 and -39 mV respectively, which are comparable to previous work.[10]) and then mixed it with CNC aqueous suspension (Thus prepared solution is denoted as S1). The other route is adding GO powder directly into CNC aqueous suspension (denoted as S2). Because only a very small amount of GO solution and powder is added to CNC suspensions for preparing 0.3 wt% GO/CNC solutions, the concentration of H^+ in CNC dispersions has hardly changed. Therefore, the pH values of resulted GO/CNC solutions (S1 and S2) are basically identical, both around 2.1. Besides, it is found that the pH of S1 and S2 did not show time-dependent changes.

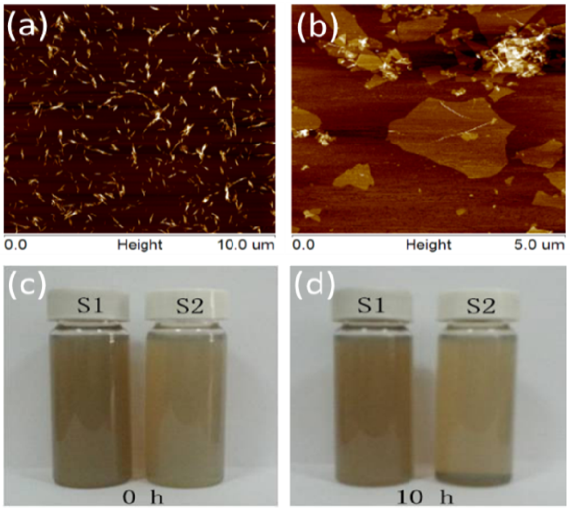

Figure 1. AFM images of CNC (a) and GO (b) particles spin-coated on mica substrate. The stability of GO/CNC solutions prepared by various sampling procedures as illustrated in Scheme 1 (denoted as S1 and S2) are compared by the optical photos taken immediately (c) and 10 hours later (d) after sonication mixing.

For both cases, long time ultrasonic treatment (ca. 12h) was used for promoting the homogeneous dispersion of GO in CNCs aqueous solution. After that, it seems that homogenous mixtures are obtained for both S1 and S2 (see Fig. 1c). However, it is found that S1 remains stable for long time, whereas S2 just stable for several hours. As evidenced by optical photos in Fig 1d, the appearance of S1 is still homogenous after stored for 10 h, while some precipitate appears at the bottom of the bottle for S2. This observation suggests that the dispersibility of GO in CNC aqueous solution is different for these two sampling methods. In fact, it is well known that GO can be well exfoliated and dissolved in neutral water.[11] Moreover, both GO and CNC are negatively charged in aqueous solution. Therefore, it is reasonable to find that mixture of GO and CNC aqueous solutions could form homogenous and stable colloidal dispersion. Nevertheless, completely exfoliation of GO powder in CNC aqueous solution with pH = 2 may be difficult to be reached even with long time ultrasonic treatment. This speculation is supported by the data of dynamic light scattering. Fig. 2a shows that only one peak cantered around 200 nm is observed for S1, whereas two peaks related to the sizes of CNC and GO are respectively identified for S2. The generation of a single Gaussian DLS peak by the dispersion of polydisperse rod-like CNC and GO flakes for S1 in Figure 2a is surprising.

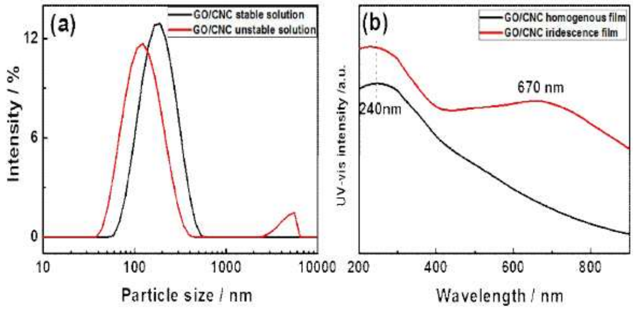

Figure 2. (a) Dynamic light scattering of stable (S1) and unstable (S2) CNC solution. (b) UV-vis absorption spectra of vacuum-filtered GO/CNC homogenous film and iridescent film.

As shown in the support information (see Fig. S1), AFM data for the stable GO/CNC solution reveal that GO flakes with lateral size of about 100-300 nm were dispersed with the CNC rods after long time ultrasonic treatment. The lateral sizes of GO sheets is roughly in the dimension range of CNC nanorods, which is consistent with the single peak Gaussian distribution in DLS for S1. Moreover, this AFM data suggest that there is no strong interaction between CNC and GO at acid condition. The small peak corresponding to large size (ca. 3-5 μm) clear suggests that some unexfoliated or aggregated GO sheets exist in S2. Therefore, sonication for S2 just produces metastable colloid dispersion.

In order to avoid further aggregation during the storage period, both S1 and S2 are immediately vacuum filtered through a PTFE filter paper (50 mm diameter, 0.22 μm pore size) after stopping the ultrasonic treatment. Finally, free-standing GO/CNC films were fabricated by peeling off from the filter paper after vacuum drying. As demonstrated in Scheme 1, the resulted GO/CNC film from stable solution shows pale yellow, whereas the film corresponding to the unstable solution demonstrates the iridescent color. For convenience, films obtained from S1 and S2 solution were represented by F1 and F2, respectively. Generally, the appearance of iridescent color indicates that the self-assembled liquid crystal phase is established in the CNC-based composite film. Because CNCs film with chiral nematic structure can selectively reflect circularly polarized light, the UV-vis spectra were collected for F1 and F2. In both samples, there is a peak around 240 nm, which is associated with the GO component. However, F2 demonstrates another peak around 670 nm. This observation suggests that the iridescent color in F2 does come from self-assembled liquid crystal phase of CNCs.

Fig. 3a and b show the morphology characterization of polarized optical microscopy (POM) in transmission mode for F1 and F2, respectively. Compared with featureless morphology of F1, the strong birefringence signal appearing in F2 gives more direct evidence that liquid crystal phase of CNCs occurs in F2.

For understanding the internal structure for F1 and F2 in detail, their fracture surface was examined by scanning electron microscopy (SEM). As shown in Fig. 3c-f, viewing the fractures from parallel to the surface of the films, F1 and F2 demonstrate clear differences not only at submicrometer but also at nanoscale structural levels. Closer look at the cross sections of the films (see Figure 3e and 3f) clearly reveals that CNC nanorod and GO sheet contact intimately and distributed uniformly in the fracture surface. However, totally different self-organized structure is observed for F2. Firstly, there is layered stacking structure, in which the repeating distance is of the order of several hundred nanometers as denoted by the white parallel lines of dashes in Fig. 3f. Secondly, it is found that aggregated GO sheets (marked by the white cycle in Fig. 3f) are embedded in the ordered self-assembly structure of CNC. In general, classic helical model of cholesteric liquid crystal has often been used to explain the structural origin of CNC iridescent films.[12] Therefore, two structural models for various self-assembly behavior of F1 and F2 are proposed in Fig. 3g and 3h, respectively.

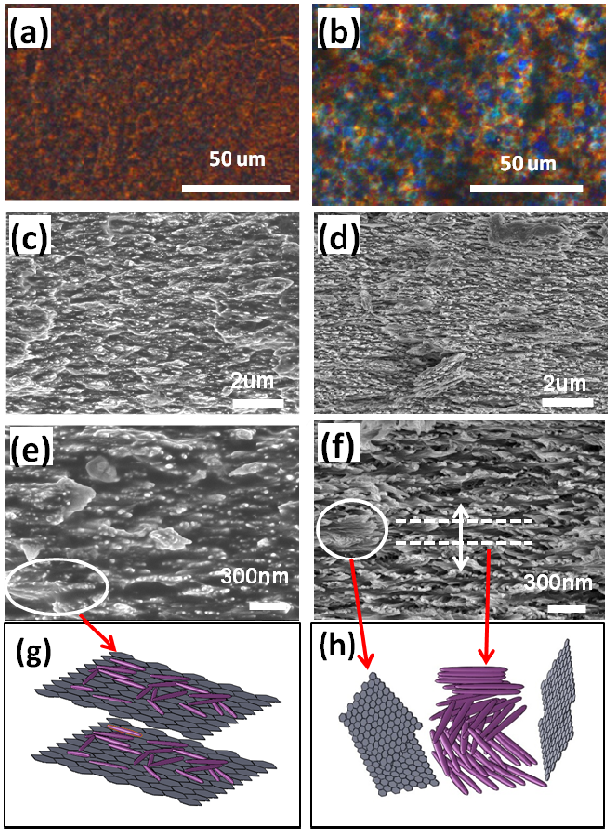

Figure 3. Comparison of optical and fracture morphology of homogeneous and iridescent CNC/TRG composite film. (a) and (b) POM image with scale bar, 20 μm. The micrograph was taken with crossed polarizer; (c) and (d) SEM images of a fracture surface across the composite film (scale bar, 20 μm); (e) and (f) with higher magnification (scale bar, 300 nm). The self-assembling structures in homogeneous and iridescent CNC/TRG composite film are depicted in (g) and (h), respectively.

To obtain both optical and conductive CNC-based materials, chemical reduction process was performed on both CNC/GO films with hydrazine vapour at 50 ˚C for 18 hours.[11] The marked changes in colour before and after reduction (Fig. 4a) indicates that GO in both films were successfully reduced into graphene (RGO). The reduced F1 and F2 films (I and II) respectively show the dark colour and iridescent colour, when illuminated by white light. It suggests that the chiral liquid crystal phase in F2 keeps intact during chemical reduction process. The conductivity values measured by a Sourcemeter are shown in Fig. 4c. The conductivity of CNC/RGO no-iridescent film can reach 5.4×10^{-2} S • m^{-1}, with GO content only 0.3 wt%. However, the conductivity of CNC/RGO iridescent film shows 5.7×10^{-5} S • m^{-1}. The iridescent CNC/RGO film shows certain electrical conductivity although its conductive performance is inferior to that of the no-iridescent one. It is not difficult to understand the difference between the conductivity of these two films. As mentioned above. GO sheets dispersed homogeneously in the CNC/GO stable solution so that the resulted film demonstrates excellent electronic properties. Nevertheless, nonuniform incorporation of GO aggregate in self-assembled liquid crystal of CNC leads to poor conductivity.

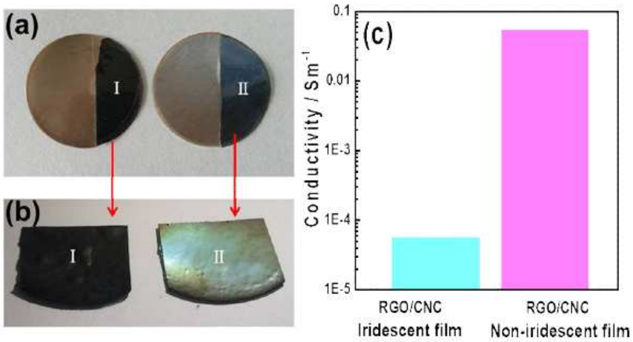

Figure 4. Optical photos: (a) F1 and F2 film before and after reduction by hydrazine vapour. The yellow part is the original one, and the dark part is reductive. I and II represent the reduced films from F1 and F2, respectively. (b) Comparison of the color for reductive F1 and F2 film illuminated by white light; (c) Conductivity properties of 0.3 wt% RGO/CNC film.

The influences of GO content on optical and conductivity properties of the resulted RGO/CNC films have also been investigated (see Fig S2a and 2b). The results show that, for the hybrid films prepared from metastable solution, when the GO content was increased to 2.0%, the obtained film shows non-iridescence. Here, as iridescent is a kind of structural colour that connected with the liquid crystal self-assembly of CNCs, therefore, we infer that self-assembly of CNCs behaviour may be disturbed when GO content is above 2.0%. Unexpected, the electrical conductivity for both types of RGO/CNC composites are comparable when GO content is above 0.5 wt%. This observation suggests that conductive channel is formed for both types RGO/CNC composites at higher GO content.

Conclusions

In summary, two distinguished GO/CNC hybrid films with various internal structure and functional properties have been obtained by controlling the dispersibility of GO in CNC aqueous solution. When the film is self-organized from stable GO/CNC solution with VASA technique, homogenous mixing of CNC rod and GO sheet at nanoscale could be realized. However, the GO/CNC film from metastable solution demonstrates phase separated structure. Interestingly enough, UV-vis, POM and SEM data clearly suggest that the phase separated structure consists of self-assembled liquid crystal phase of CNC with embedded GO sheets. The self-assembled liquid crystal phase endowed the resulted GO/CNC film with iridescent optical properties, which is well kept even suffered through the treatment of chemical reduction. To the best of our knowledge, it is the first time to report the large size, crack free and iridescent GO/CNC hybrid film fabricated by VASA. We anticipate that the iridescent films prepared through our method have potential applications in photonic materials for large-scaled and intact needs, sensors, tunable and reflective filters, security materials and so on.

Admittedly, still much effort is needed to understand the liquid crystal self-assembly behaviour of CNC under flow field and the functional properties of GO/CNC composite films.

The authors acknowledge the financial support from Taishan Mountain Scholar Foundation (TS20081120), and Natural Science Fund for Distinguished Young Scholars of Shandong Province (JQ200905) are greatly appreciated.

Notes and references

Key Laboratory of Rubber-Plastics, Ministry of Education/
Shandong Provincial Key Laboratory of Rubber-plastics, Qingdao University of Science & Technology, Qingdao City 266042, People's Republic of China. Fax: +86 532 84022791; Tel: +86 532 84022604; E-mail: dyx@qust.edu.cn (Y.D.); zjm@qust.edu.cn (J. Z.)

1 a) Y. Habibi, L. A. Lucia and O. J. Rojas, *Chemical reviews*, 2010, **110**, 3479; b) D. Klemm, F. Kramer, S. Moritz, T. Lindström, M. Ankerfors, D. Gray, A. Dorris, Angew. Chem. Int. Ed. 2011, 50, 5438; c) R. J. Moon, A. Martini, J. Nairn, J. Simonsen and J. Youngblood, *Chem Soc Rev*, 2011, **40**, 3941.

2 a) J. J. Blaker, K. Y. Lee, A. Bismarck, *J Biobased Mater Bio,* 2011, **5,** 1. b) X. Cao, H. Dong and C. Li, *Biomacromolecules,* 2007, **8**, 899.

3 J. P. Lagerwall, C. Schütz, M. Salajkova, J. Noh, J. H. Park, G. Scalia and L. Bergström, *NPG Asia Materials*, 2014, **6(1)**, e80.

4 a) K. E. Shopsowitz, H. Qi, W. Y. Hamad and M. J. MacLachlan, *Nature*, 2010, **468**, 422. b) K. E. Shopsowitz, W. Y. Hamad and M. J. MacLachlan, *J. Am. Chem. Soc,* 2012, **134**, 867. c) K. E. Shopsowitz, A. Stahl, W. Y. Hamad, and M. J. MacLachlan, *Angew Chem Int Ed.*2012, **51**, 6886.

5 J. A. Kelly, A. M. Shukaliak, C. C. Cheung, K. E. Shopsowitz, W. Y. Hamad and M. J. MacLachlan, *Angew Chem Int Ed*. 2013, **52**, 8912.

6 J. A. Kelly, M. Giese, K.E. Shopsowitz, W. Y. Hamad and M. J. MacLachlan, *Acc. Chem. Res*, 2014, **47**, 1088.

7 a) X. M. Dong, T. Kimura, J. –F. Revol and D. G. Gray, *Langmuir*, 1996, **12**, 2076. b) S. Beck, J. Bouchard and R. Berry, *Biomacromolecules*, 2011, **12**, 167. c) S. Beck, J. Bouchard, G. Chauve and R. Berry, *Cellulose*, 2013, **20**, 1401. d) T. D. Nguyen, W. Y. Hamad and M. J. MacLachlan, *Chem. Commun*, 2013, **49**, 11296.

8 C. C. Cheung, M. Giese, J. A. Kelly, W. Y. Hamad and M. J. MacLachlan, *ACS Macro Letters*, 2013, **2**, 1016.

9 W. S. Hummers, R. E. Offerman, *J. Am. Chem. Soc,* 1958, **80**, 1339.

10 D. Li, M. B. Müller, S. Gilje, R. B. Kaner and G. G. Wallace, *Nature nanotechnology*, 2008, **3**, 101.

11 H. A. Becerril, J. Mao, Z. Liu, R. M. Stoltenberg, Z. Bao, Y. Chen, *ACS Nano*, 2008, **2**, 463

12 E. Sackmann, S. Meiboom, L. C. Snyder, *J. Am. Chem. Soc,* 1968, **90**, 3567.